Integrated photonic sources of frequency-bin-encoded multipartite entangled states

Milica Banic ,[1,*] J. E. Sipe,[1] and Marco Liscidini [2]

[1]*Department of Physics, University of Toronto, 60 St. George Street, Toronto, Ontario, Canada M5S 1A7*
[2]*Department of Physics, University of Pavia, Via Bassi 6, 27100 Pavia, Italy*

We demonstrate that genuine multipartite entangled states can be generated using frequency bin encoding in integrated photonic platforms. We introduce a source of four-photon GHZ states and a source of three-photon W states. We predict generation rates on the order of 10^4 Hz for a silicon microring source with milliwatt pump powers. These results, along with the versatility and scalability of integrated structures, identify this as a promising approach for the generation of higher-dimensional and larger entangled states.

I. INTRODUCTION

Entangled states are an indispensible resource for a host of quantum protocols and for tests of fundamental physics. There is now an abundance of photonic sources of bipartite entangled states and strategies for generating multipartite states are being explored [1]. Multipartite entangled states, which exist in a Hilbert space with three or more factor spaces, are particularly interesting from both a fundamental and practical point of view: they exhibit correlations that cannot be reproduced with only bipartite states.

Multipartite states can be encoded in a number of ways, including using multiple degrees of freedom in only two particles [2]. However, many applications rely on *genuine* multipartite entangled states [3,4]; we define genuine multipartite states as those for which the Hilbert state is composed of *n* factor spaces which correspond to *n* physically separable entities, for example, *n* photons.

Genuine multipartite states can be composed of photons generated by parametric nonlinear processes, such as spontaneous four-wave mixing (SFWM) or spontaneous parametric down-conversion. The logical states can be encoded in a number of ways. Many approaches make use of polarization encoding in bulk systems [5,6], but this scheme has drawbacks: it is constrained to two logical states per particle—e.g., horizontal or vertical polarization—and it lacks scalability, since polarization is difficult to control in integrated systems.

Motivated by the need for integration, path encoding has also been explored. In this scheme, the logical state is encoded by the waveguide in which the photon is detected [7,8]. Although this can be implemented on-chip [9], its scalability is challenging because increasing the dimensionality of the system requires increasing the number of waveguides. In some cases, the implementation of large states is also complicated by the need to avoid waveguide crossings, at least for conventional lithography processes.

Another approach is energy encoding, where information is encoded in the photons' frequencies. This degree of freedom is scalable, robust, and compatible with integrated platforms. Taking photons generated by SFWM, one possibility is to encode the logical states in the generated photons' frequencies, red- or blue-detuned with respect to the pump. This scheme has been implemented in bulk for the generation of energy-encoded W states [10] and it can in principle be extended to integrated structures [11]. However, the relatively large spacing between the logical states' frequencies makes their manipulation challenging.

Recently, frequency bin encoding has been explored. This is a type of energy encoding in which the frequencies are close enough to be manipulated using commercial electro-optic modulators (EOMs) [12]. It has been demonstrated that more than two logical states could be implemented in this approach, making frequency bin encoding a promising candidate for the generation of qudit states [12,13]. The generation of frequency-bin-encoded states can be implemented using photons generated by SFWM in a resonator, in which the photon pairs are generated in a comb of resonances [14–16]. In this scheme, the logical state of a photon is determined by its spectral distance from the pump resonance (see Fig. 1).

The generation of frequency-bin-encoded bipartite entangled states, such as Bell states, has already been demonstrated [17]; in the present work, we discuss the generation of frequency-bin-encoded multipartite states in integrated photonic devices. We demonstrate how this strategy can be used for the generation of W states and GHZ states, two paradigmatic examples of multipartite entangled states. In Sec. II we describe the multiphoton sources employed in these devices. In Sec. III we discuss the generation of four-photon GHZ states and in Sec. IV we do the same for three-photon W states. Finally, we draw our conclusions in Sec. V.

II. PHOTON SOURCES

The schemes to be discussed begin with the generation of entangled photons by spontaneous four-wave mixing (SFWM) in ring resonators. We assume that the sources generate uncorrelated photon pairs; this can be accomplished

*Present address: National Research Council of Canada, 100 Sussex Drive, Ottawa, Ontario K1A 0R6, Canada; Milica.Banic@nrc-cnrc.gc.ca
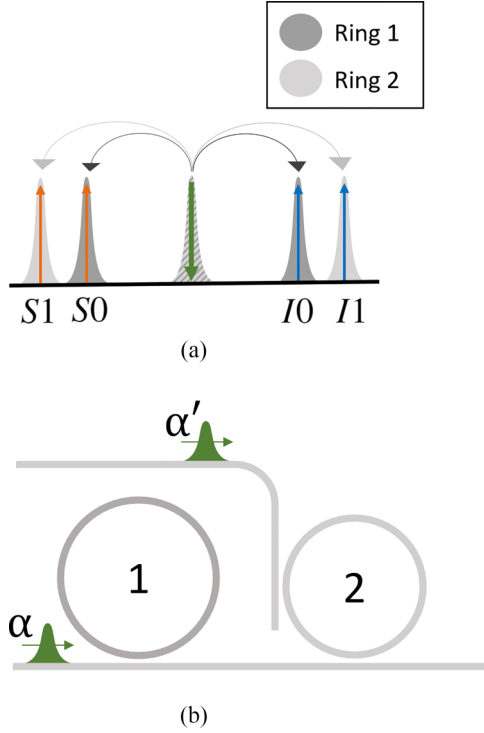
FIG. 1. Single-pump configuration described by Eq. (1). The configuration of the different modes in frequency is sketched in (a). Green arrows represent classical pumps (with amplitudes α, α'); orange and blue arrows represent signal and idler fields. $S0$, $S1$, $I0$, $I1$ label the ring resonances. The source and the pumping scheme is shown in (b).

by driving the microring source with appropriately shaped pulses [18] or by using more complex ring resonator structures as the source [19]. Here we will assume the sources are driven by a train of pulses with a duration shorter than the dwelling time of the ring resonators. Under these conditions the generated photon pairs are nearly uncorrelated [20,21] and to good approximation the photons are generated in a single Schmidt mode.

We consider two configurations for the pump and generated modes: in the first, a pump field centered at a single resonance frequency is used to generate photons in two pairs of ring resonances. Taking the generated pairs to be uncorrelated, the nonlinear Hamiltonian for this pumping scheme can be written as

$$H_{\mathrm{NL}}(t) = \hbar\Gamma\alpha^2(t)a_{S0}^\dagger a_{I0}^\dagger + \hbar\Gamma'\alpha'^2(t)a_{S1}^\dagger a_{I1}^\dagger + \mathrm{H.c.}, \quad (1)$$

where Γ and Γ' are nonlinear coupling rates, $\alpha(t)$ and $\alpha'(t)$ are pump amplitudes, and $a_J^\dagger$ is the raising operator associated with the resonance labeled by J. Each resonance has two labels associated with it: the frequency bin is denoted by a number (0 or 1), while S and I stand for signal and idler. The logical state of a photon is encoded in the frequency bin (0 or 1), which depends only on its spectral distance from the pump, but the photons also have a second label (S or I) that depends on whether they are red- or blue-shifted with respect to the pump. In this source, energy conservation ensures that pairs of signal and idler photons are generated in the same frequency bin. The frequency bins should be close enough in

frequency (10 GHz spacing) to be modulated by commercial electro-optic modulators. This constraint is important even if EOMs are not necessary for the generation of the state; their use could be necessary off-chip, for example, for the tomography of the generated state.

Equation (1) can be implemented using a single ring, provided the free spectral range is sufficiently small that the photons' frequency bins can be modulated using commercial electro-optic modulators [12]. If a single ring were used, the coefficients α and α' in Eq. (1) would be the same. Another approach is the use of two rings with different radii [15], such that each is driven by the same pump frequency, with one ring generating photon pairs in the resonances $S0$ and $I0$, while the other generates photon pairs in $S1$ and $I1$ frequencies (see Fig. 1). In this dual-ring implementation, the pump coefficients α and α' can be controlled independently. Also, if two rings are used, the distance between the frequency bins does not depend on the rings' FSR, so the frequency bins can be spectrally close without affecting the generation rate, which scales quadratically with the FSR [22]. The two rings could also be driven by a different pump amplitude and phase—hence the distinction between $\alpha(t)$ and $\alpha'(t)$ in Eq. (1).

We will also consider a dual-pump scheme (see Fig. 2), such that the generation of photons is described by

$$H_{\mathrm{NL}} = \hbar\Gamma\alpha^2(t)a_{S0}^\dagger a_{I1}^\dagger + \hbar\Gamma'\alpha'^2(t)a_{S1}^\dagger a_{I0}^\dagger + \mathrm{H.c.}, \quad (2)$$

where again we have assumed the state of the photon pairs is approximately separable. Here energy conservation requires that one photon of each pair is generated in frequency bin 1, while the other is generated in bin 0. Unlike in the previous configuration, α and α' refer to pump amplitudes at different
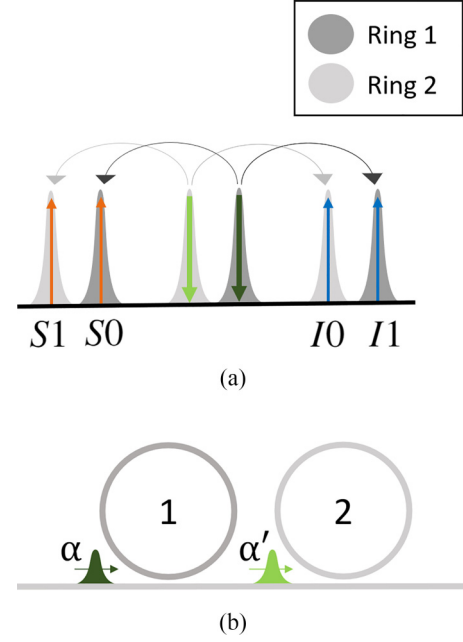

FIG. 2. Dual-pump configuration described by Eq. (2). The configuration of the modes in frequency is sketched in (a). Green arrows represent classical pumps (with amplitudes α, α'); orange and blue arrows represent signal and idler fields. $S0$, $S1$, $I0$, $I1$ label the ring resonances. The source and pumping scheme is shown in (b).
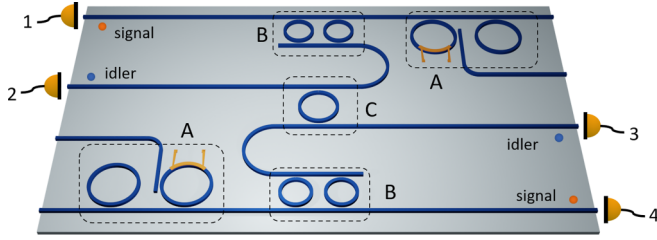
FIG. 3. Sketch of the GHZ state source. The boxes A label the photon pair sources, which are pumped as indicated in Fig. 1. For each source, the positions of the two rings' resonances can be tuned using a heater, sketched in yellow. The generated signal and idler photons are separated by demultiplexers (labeled B). C labels an add-drop filter resonant with frequency bin $I1$.

frequencies, so they could be made distinct even in an implementation with a single ring. However, two high-finesse rings could be used to increase the generation rate [16].

For each cycle in the pulse train, the state generated in either pumping scheme can be written as

$$|\psi\rangle = e^{-\frac{i}{\hbar}\int_{t_0}^{t} dt' H_{\mathrm{NL}}(t')} |\mathrm{vac}\rangle, \qquad (3)$$

where we have neglected time ordering corrections. Inserting Eq. (1) or (2), we can write

$$|\psi\rangle = e^{\beta C_{II}^{\dagger}-\mathrm{H.c.}} |\mathrm{vac}\rangle, \qquad (4)$$

where $C_{II}^{\dagger}$ is a pair generation operator. We will consider the parameter regime where, to good approximation, at most four photons are generated in each cycle, with the probability of higher-order events being negligible. In this case (4) can be approximated as

$$|\psi\rangle \approx [1 + \mathcal{O}(\beta^2)] |\mathrm{vac}\rangle + \beta C_{II}^{\dagger} |\mathrm{vac}\rangle + \frac{\beta^2}{2} C_{II}^{\dagger 2} |\mathrm{vac}\rangle, \quad (5)$$

where $C_{II}^{\dagger} |\mathrm{vac}\rangle$ is a normalized two-photon state and $|\beta|^2$ is the probability of generating a photon pair per pump pulse, in the low pair generation regime [7,11,23].

III. FOUR-PHOTON GHZ STATES

We first discuss the generation of frequency-bin-encoded four-photon Greenberger-Horne-Zeilinger (GHZ) states. A maximally entangled four-qubit GHZ state has the form

$$|\mathrm{GHZ}\rangle = \frac{1}{\sqrt{2}}(|0000\rangle + |1111\rangle), \qquad (6)$$

where 0 and 1 denote the qubits' logical states. GHZ states are resources for tasks ranging from fundamental tests of quantum mechanics to applications in quantum information and communication [3,24–26].

The source of frequency-bin-entangled GHZ states is sketched in Fig. 3. The scheme implemented by this device is analogous to the one implemented in bulk systems for the generation of polarization-encoded GHZ states [5] and it relies on postselection on fourfold coincidences.

In our implementation, we begin with the generation of photon pairs in two microring sources in the single-pump configuration (labeled "A" in Fig. 3). We assume all four rings

are driven simultaneously to generate photons that are indistinguishable in time; in Fig. 3 we envision splitting the pump such that each ring is coupled to its own input waveguide.

The state generated by each source is described by Eq. (5). Inserting Eq. (1) in (3) we have

$$C_{II}^{\dagger} = \frac{1}{\beta}\{\beta_1 a_{S0}^{\dagger} a_{I0}^{\dagger} + \beta_2 a_{S1}^{\dagger} a_{I1}^{\dagger}\}, \qquad (7)$$

where

$$\beta_1 = -i\Gamma \int_{t_0}^{t} \alpha^2(t')dt', \qquad (8)$$

$$\beta_2 = -i\Gamma' \int_{t_0}^{t} \alpha'^2(t')dt' \qquad (9)$$

are related to the probabilities of generating a pair of photons in each pair of resonances ($S0$ and $I0$ or $S1$ and $I1$) and $|\beta|^2 = |\beta_1|^2 + |\beta_2|^2$ is again the total probability of generating a photon pair per pump pulse. The state generated by each source then is

$$|\psi\rangle = |\mathrm{vac}\rangle + (\beta_1 a_{S0}^{\dagger} a_{I0}^{\dagger} + \beta_2 a_{S1}^{\dagger} a_{I1}^{\dagger}) |\mathrm{vac}\rangle, \qquad (10)$$

where we have restricted our attention to the first-order term. In principle, four photons can be generated in a single source. However, our postselection on signal photons prevents such events from causing fourfold coincidences.

The signal and idler photons from each source are separated deterministically using a series of add-drop filters, which act as a dichroic mirror ("B" in Fig. 3). Paths 1 and 4 carry only signal photons, while paths 2 and 3 carry only idler photons. All four paths carry both logical states, because the logical state and signal or idler are distinct degrees of freedom in this encoding. At this stage the state can be written as

$$|\psi\rangle = \left[|\mathrm{vac}\rangle + \left(\beta_1 a_{S0}^{\dagger(1)} a_{I0}^{\dagger(2)} + \beta_2 a_{S1}^{\dagger(1)} a_{I1}^{\dagger(2)}\right) |\mathrm{vac}\rangle\right]$$
$$\otimes \left[|\mathrm{vac}\rangle + \left(\beta_3 a_{S0}^{\dagger(4)} a_{I0}^{\dagger(3)} + \beta_4 a_{S1}^{\dagger(4)} a_{I1}^{\dagger(3)}\right) |\mathrm{vac}\rangle\right], \quad (11)$$

where the superscript on each ladder operator denotes the relevant path (see Fig. 3). Expanding the tensor product results in zero-, two-, and four-photon terms; we restrict our attention to the latter, since fourfold coincidence events will be postselected. The relevant term is

$$|\psi_{IV}\rangle = \mathcal{N}\left(\beta_1 a_{S0}^{\dagger(1)} a_{I0}^{\dagger(2)} + \beta_2 a_{S1}^{\dagger(1)} a_{I1}^{\dagger(2)}\right) |\mathrm{vac}\rangle$$
$$\otimes \left(\beta_3 a_{S0}^{\dagger(4)} a_{I0}^{\dagger(3)} + \beta_4 a_{S1}^{\dagger(4)} a_{I1}^{\dagger(3)}\right) |\mathrm{vac}\rangle, \qquad (12)$$

where $\mathcal{N}$ is a normalization constant.

Next, paths 1 and 4 are routed to detectors, while paths 2 and 3 are "merged" at an add-drop filter resonant with $I1$, but not $I0$ ("C" in Fig. 3). The add-drop acts in analogy to a polarizing beam splitter, effecting the transformation

$$a_{I0}^{\dagger(2)} \rightarrow a_{I0}^{\dagger(2)},$$
$$a_{I0}^{\dagger(3)} \rightarrow a_{I0}^{\dagger(3)},$$
$$a_{I1}^{\dagger(2)} \rightarrow a_{I1}^{\dagger(3)},$$
$$a_{I1}^{\dagger(3)} \rightarrow a_{I1}^{\dagger(2)}. \qquad (13)$$

Because we will trace over S and I, paths 2 and 3 must contain photons of the same color to obtain a pure GHZ state. The

state following the add-drop is

$$\begin{aligned}|\psi_{IV}\rangle = \mathcal{N}\big(\beta_1 a_{S0}^{\dagger(1)} a_{I0}^{\dagger(2)} + \beta_2 a_{S1}^{\dagger(1)} a_{I1}^{\dagger(3)}\big)|vac\rangle \\ \otimes \big(\beta_3 a_{S0}^{\dagger(4)} a_{I0}^{\dagger(3)} + \beta_4 a_{S1}^{\dagger(4)} a_{I1}^{\dagger(2)}\big)|vac\rangle,\end{aligned} \quad (14)$$

and the state describing fourfold coincidence events is

$$\begin{aligned}|\bar{\psi}_{IV}\rangle = \bar{\mathcal{N}}\big(\beta_1\beta_3 a_{S0}^{\dagger(1)} a_{I0}^{\dagger(2)} a_{I0}^{\dagger(3)} a_{S0}^{\dagger(4)} \\ + \beta_2\beta_4 a_{S1}^{\dagger(1)} a_{I1}^{\dagger(2)} a_{I1}^{\dagger(3)} a_{S1}^{\dagger(4)}\big)|vac\rangle\end{aligned} \quad (15)$$

$$= \bar{\mathcal{N}}(\beta_1\beta_3|0000\rangle + \beta_2\beta_4|1111\rangle)|SIIS\rangle, \quad (16)$$

which is a pure frequency-bin-encoded GHZ state after tracing over S and I.

We envision the source in Fig. 3(a) to be a pair of silicon microring resonators. Such sources have been shown to generate nearly uncorrelated photon pairs with $|\beta|^2 \approx 0.1$ for picojoule pump pulses with durations around 10 ps and a 10 MHz repetition rate; this corresponds to a pair rate of $\sim 10^6$ Hz [20]. From this we predict the probability of generating a pair of pairs per pump pulse to be $\sim |\beta|^4 \approx 0.01$, giving a four-photon generation rate $\mathcal{R}_{IV} \sim 10^5$ Hz. Half of these sets of photons lead to fourfold coincidences after the add-drop (see the Appendix), so we expect a GHZ generation rate of 10^4–10^5 Hz for milliwatt pump powers. The expected off-chip rate depends strongly on the coupling loss, which is strongly dependent on the platform chosen for the implementation of the circuit. As an example, if one assumes a coupling loss of 6 dB per channel, which has been reported in recent work on a silicon platform [16], the expected fourfold coincidence rate would be on the order of 10–100 Hz.

This scheme could be modified to produce a three-photon GHZ state by choosing one of the four paths to be an ancilla and using an EOM in this path to shift photons in bin 0 to 1 or vice versa. That is, the EOM would modify the state to be

$$|\bar{\psi}_{IV}\rangle = \bar{\mathcal{N}}(\beta_1\beta_3 e^{-i\phi}|0001\rangle + \beta_2\beta_4|1111\rangle)|SIIS\rangle, \quad (17)$$

a three-photon GHZ state with an ancilla photon in path 4. By ϕ we denote the phase acquired due to the modulation; the pump phases could be adjusted to cancel this out.

Given the relative ease of implementing more than two logical states in frequency bin encoding, one might think about extending this scheme to higher dimensions. Yet, this device cannot be simply generalized to generate high-dimensional four-photon GHZ states and it is unclear whether such a source could be implemented using this platform with only four photons. This sort of extension is challenging in general and we comment on this more in the Conclusion.

IV. THREE-PHOTON W STATES

We now turn to the generation of three-photon W states. W states are known to be relatively robust against loss [27] and, like GHZ states, they have been explored as resources for a number of quantum protocols [28–33]. A maximally entangled three-qubit W state has the form

$$|W\rangle = \frac{1}{\sqrt{3}}(|100\rangle + |010\rangle + |001\rangle). \quad (18)$$

Our scheme for generating such states begins with the generation of four photons in a single source (labeled "A" in
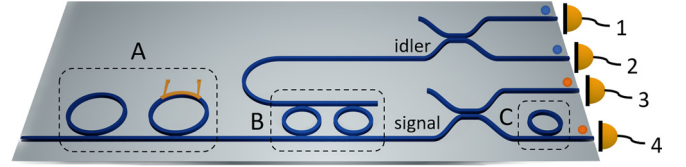

FIG. 4. Integrated W state source. Box A labels the photon source, which is pumped as indicated in Fig. 2. The heater sketched in yellow can be used to tune the positions of the two rings' resonances. Signal and idler photons are separated at the demultiplexer (B) and routed toward detectors. C labels a filter which transmits only signal photons in frequency bin 1.

Fig. 4) with the pumping scheme sketched in Fig. 2. In this case the two rings' resonances are different and they can be excited simultaneously through the same bus waveguide and a properly engineered pump.

Here

$$C_{II}^\dagger = \frac{1}{\beta}\{\beta_1 a_{S0}^\dagger a_{I1}^\dagger + \beta_2 a_{S1}^\dagger a_{I0}^\dagger\}, \quad (19)$$

with β_1 and β_2 defined in Eqs. (8) and (9). Inserting this in Eq. (5) and restricting our attention to the four-photon terms, we have

$$\begin{aligned}|\psi_{IV}\rangle = \mathcal{N}\big(\beta_1^2 a_{S0}^\dagger a_{S0}^\dagger a_{I1}^\dagger a_{I1}^\dagger + \beta_2^2 a_{S1}^\dagger a_{S1}^\dagger a_{I0}^\dagger a_{I0}^\dagger \\ + 2\beta_1\beta_2 a_{S0}^\dagger a_{S1}^\dagger a_{I0}^\dagger a_{I1}^\dagger\big)|vac\rangle.\end{aligned} \quad (20)$$

As in the GHZ device, the signal and idler photons are separated deterministically by add-drop filters ("B" in Fig. 4); the signal photons are routed to path 4 and the idler photons to path 2. Each path is sent into a directional coupler (DC) which acts as a 50-50 beam splitter. Three of the four DC outputs lead directly to detectors: these are the three "parties" among which the W state is shared. The fourth output (path 4) is filtered ("C" in Fig. 4), leaving only photons generated in resonance $S1$, and then routed to a herald detector. After this processing, a four-photon coincidence event is described by

$$|IV'\rangle = \mathcal{N}'\big[4\beta_2^2|0011\rangle + 2\beta_1\beta_2(|0101\rangle + |1001\rangle)\big]|IISS\rangle, \quad (21)$$

which is derived in Appendix.

Here again we expect the rate of pairs of pairs generated in the source to be $\sim 10^5$ Hz (see Sec. III). The fraction of four-photon sets that could lead to fourfold coincidences after the DCs and filtering in path 4 is given by

$$\mathcal{F} = \frac{1}{8}\left(\frac{2|\beta_2|^4 + |\beta_1|^2|\beta_2|^2}{|\beta_1|^4 + |\beta_2|^4 + |\beta_1|^2|\beta_2|^2}\right), \quad (22)$$

where we have set $\mathcal{R} = \mathcal{T} = \frac{1}{\sqrt{2}}$ for the DCs, which should be configured as 50-50 beam splitters to maximize the generation rate. The total rate of W states is $\mathcal{R}_W = \mathcal{F}\mathcal{R}_{IV}$. The rate depends on the relative amplitudes of β_1 and β_2; for example, to generate the W state of Eq. (18), one would set $\beta_1 = 2\beta_2$, giving $\mathcal{F} = \frac{1}{28}$. Then with a silicon microring source we estimate $\mathcal{R}_W \sim 10^3$–10^4 Hz for milliwatt pump powers.

We point out that the redundant degree of freedom can be exploited to improve the efficiency: without the signal or idler label, the photons could not be deterministically separated

into two multiple paths, so the fraction of photons leading to fourfold coincidences would be smaller. Indeed, in this respect, this scheme is more efficient than a similar scheme where the signal or idler labels *do* encode the logical states, with three beam splitters required to route them to four detectors [10,11].

This device cannot be generalized directly as a source for N-photon W states with $N > 3$: for $N > 4$, one would require more photon pairs distributed among more paths, so the form of the circuit would immediately need to be modified. Since the source in this device always generates an equal number of photons in bin 0 and bin 1, an $N = 4$ W state would require either a different source or the use of ancillas, which would again require more sources and paths. The design of other sources for larger W states is an interesting area for future work and it is possible that a more general design or approach could be found.

V. CONCLUSION

Frequency bin encoding has emerged as a convenient approach to the generation of nonclassical light, particularly in integrated platforms. The generation of high-fidelity Bell states, for example, has been demonstrated; here we have explored the generation of multipartite states. We have described integrated sources of frequency-bin-encoded W and GHZ states, based on the manipulation and postselection of photon pairs generated by SFWM in pulsed microring sources. For typical silicon microring sources pumped by picojoule pump pulses with a MHz repetition rate, we predict generation rates of 10^3–10^4 Hz for both W and GHZ states. The implementation of these schemes is a clear next step in extending frequency bin encoding towards the generation of multipartite entangled states.

Frequency bin encoding can accommodate more than two logical levels and integrated platforms are well-suited for multiplexing many photon sources; it is natural to consider whether one could conceive sources of more complex, high-dimensional multipartite states. The schemes discussed here cannot be generalized in a straightforward way, a difficulty that has been encountered by others [34]. It is challenging to comment more generally on the resources required to generate a particular state or, conversely, about what states can be generated given a particular set of experimental resources. Indeed, it has been demonstrated that one cannot even efficiently compute the high-dimensional state generated by a given experimental scheme [35]. Yet the extension of this work to the design of more complex sources is an obvious topic for future work, especially given the ease with which—relative to other scenarios for investigating high-dimensional degrees of freedom—the platforms discussed here can be implemented.

APPENDIX: W AND GHZ DETAILS

Here we provide a more detailed description of the W and GHZ generation schemes.

1. Three-photon W state

We consider the W state device (Fig. 4) with the photon pair source driven in the dual-pump scheme (Fig. 2). Assuming that the generated photon pairs are roughly separable, the nonlinear Hamiltonian describing the production of pairs can be taken to be

$$H_{\mathrm{NL}} = \hbar\Gamma\alpha^2(t)a_{S0}^\dagger a_{I1}^\dagger + \hbar\Gamma'\alpha'^2(t)a_{S1}^\dagger a_{I0}^\dagger + \mathrm{H.c.} \quad (A1)$$

Here Γ and Γ' are nonlinear coupling rates associated with each ring, α and β are classical pump amplitudes in the two rings, and $a_J^\dagger$ are raising operators associated with a ring resonance J. Neglecting time ordering corrections, this generates the state

$$|\psi\rangle = e^{-\frac{i}{\hbar}\int_{t_0}^t dt' H_{\mathrm{NL}}(t')} |\mathrm{vac}\rangle \quad (A2)$$

$$= e^{-i\int_{t_0}^t dt'\left[\Gamma\alpha(t')^2 a_{S0}^\dagger a_{I1}^\dagger + \Gamma'\alpha'^2(t')a_{S1}^\dagger a_{I0}^\dagger + \mathrm{H.c.}\right]} |\mathrm{vac}\rangle \quad (A3)$$

$$= e^{\left\{-i\Gamma\left(\int_{t_0}^t dt'\alpha^2(t')\right)a_{S0}^\dagger a_{I1}^\dagger - i\Gamma'\left(\int_{t_0}^t dt'\alpha'^2(t')\right)a_{S1}^\dagger a_{I0}^\dagger\right\}-\mathrm{H.c.}} |\mathrm{vac}\rangle \quad (A4)$$

$$\equiv e^{\beta C_{II}^\dagger - \mathrm{H.c.}} |\mathrm{vac}\rangle, \quad (A5)$$

where we introduce the pair generation operator

$$C_{II}^\dagger = \frac{1}{\beta}\left\{-i\Gamma\left(\int_{t_0}^t dt'\alpha^2(t')\right)a_{S0}^\dagger a_{I1}^\dagger\right.$$
$$\left. -i\Gamma'\left(\int_{t_0}^t dt'\alpha'^2(t')\right)a_{S1}^\dagger a_{I0}^\dagger\right\} \quad (A6)$$

$$\equiv \frac{1}{\beta}\left\{\beta_1 a_{S0}^\dagger a_{I1}^\dagger + \beta_2 a_{S1}^\dagger a_{I0}^\dagger\right\}. \quad (A7)$$

Here $|\beta|^2 = |\beta_1|^2 + |\beta_2|^2$ is the probability of generating a pair per pump pulse and $C_{II}^\dagger |\mathrm{vac}\rangle$ is a normalized two-photon state.

We consider the regime of low pair generation probability, such that pairs of photons and pairs of pairs are generated, with negligible higher-order events. The state generated by the source then is approximately

$$|\psi\rangle = [1 + \mathcal{O}(\beta^2)]|\mathrm{vac}\rangle + \beta C_{II}^\dagger |\mathrm{vac}\rangle + \frac{\beta^2}{2}C_{II}^{\dagger 2}|\mathrm{vac}\rangle, \quad (A8)$$

which is just Eq. (A5) to second order. If we set $\beta_2 = \beta_1 e^{i\phi}$, then the two-photon term above (when normalized) corresponds to a frequency-bin-encoded Bell state of the form

$$|\Psi\rangle = \frac{1}{\sqrt{2}}(a_{S0}^\dagger a_{I1}^\dagger + e^{i\phi}a_{S1}^\dagger a_{I0}^\dagger)|\mathrm{vac}\rangle \quad (A9)$$

$$= \frac{1}{\sqrt{2}}(|01\rangle + e^{i\phi}|10\rangle), \quad (A10)$$

where the two qubits are the signal and idler photons and their logical states are encoded in the frequency bins in which they are generated.

Here we are interested in the four-photon terms that arise from the latter term in (A8). Inserting $C_{II}^\dagger$ we have

$$|\psi_4\rangle = \mathcal{N}\big(\beta_1^2 a_{S0}^\dagger a_{S0}^\dagger a_{I1}^\dagger a_{I1}^\dagger + \beta_2^2 a_{S1}^\dagger a_{S1}^\dagger a_{I0}^\dagger a_{I0}^\dagger \\ + 2\beta_1\beta_2 a_{S0}^\dagger a_{S1}^\dagger a_{I0}^\dagger a_{I1}^\dagger\big)|\text{vac}\rangle, \tag{A11}$$

where

$$\mathcal{N} = \frac{1}{\sqrt{4|\beta_1|^4 + 4|\beta_2|^4 + 4|\beta_1|^2|\beta_2|^2}} \tag{A12}$$

is a normalization constant.

a. Routing photons

We consider a setup where the signal and idler photons generated by the source are split between two paths. Each path is then split by a beam splitter and we postselect on four-photon coincidences (see Fig. 4). We can write the operators in Eq. (A11) in terms of operators referring to each detection arm using beam splitter input-output relations. Recall for a single beam splitter, where we label the input ports 1 and 2 and the output ports 3 and 4, we have

$$\begin{bmatrix} a_3 \\ a_4 \end{bmatrix} = \begin{bmatrix} \mathcal{T} & \mathcal{R} \\ \mathcal{R} & \mathcal{T} \end{bmatrix}\begin{bmatrix} a_1 \\ a_2 \end{bmatrix}, \tag{A13}$$

where the matrix is unitary. Using this we obtain

$$a_1 = \mathcal{T}^* a_3 + \mathcal{R}^* a_4, \\ a_2 = \mathcal{R}^* a_3 + \mathcal{T}^* a_4, \tag{A14}$$

so for our setup we can write

$$a_I = \mathcal{R}_1^* c_I^{(1)} + \mathcal{T}_1^* c_I^{(2)}, \\ a_S = \mathcal{R}_2^* c_S^{(3)} + \mathcal{T}_2^* c_S^{(4)}. \tag{A15}$$

Here $c_J^{(n)}$ are ladder operators associated with the output branch n (see Fig. 4). We now substitute (A15) into (A11).

The resulting expression involves operators of the form

$$\mathcal{O}_{J,J',K,K'} = a_J^\dagger a_{J'}^\dagger a_K^\dagger a_{K'}^\dagger \tag{A16}$$

acting on the vacuum, where J, J' are associated with signal photons and K, K' with idler photons. Inserting (A15) into (A16) we have

$$\mathcal{O}_{J,J',K,K'} = \big(\mathcal{R}_2 c_J^{(3)\dagger} + \mathcal{T}_2 c_J^{(4)\dagger}\big)\big(\mathcal{R}_2 c_{J'}^{(3)\dagger} + \mathcal{T}_2 c_{J'}^{(4)\dagger}\big) \\ \times \big(\mathcal{R}_1 c_K^{(1)\dagger} + \mathcal{T}_1 c_K^{(2)\dagger}\big)\big(\mathcal{R}_1 c_{K'}^{(1)\dagger} + \mathcal{T}_1 c_{K'}^{(2)\dagger}\big).$$

Expanding this we have

$$\mathcal{O}_{J,J',K,K'} = \mathcal{R}_1\mathcal{T}_1\mathcal{R}_2\mathcal{T}_2\big(c_{J'}^{(3)\dagger} c_J^{(4)\dagger} + c_J^{(3)\dagger} c_{J'}^{(4)\dagger}\big)\big(c_K^{(1)\dagger} c_{K'}^{(2)\dagger} + c_{K'}^{(1)\dagger} c_K^{(2)\dagger}\big) + \overline{\mathcal{O}}_{J,J',K,K'} \tag{A17}$$

$$= \mathcal{R}_1\mathcal{R}_2\mathcal{T}_1\mathcal{T}_2\big(c_{J'}^{(3)\dagger} c_J^{(4)\dagger} c_K^{(1)\dagger} c_{K'}^{(2)\dagger} + c_{J'}^{(3)\dagger} c_J^{(4)\dagger} c_{K'}^{(1)\dagger} c_K^{(2)\dagger} + c_J^{(3)\dagger} c_{J'}^{(4)\dagger} c_K^{(1)\dagger} c_{K'}^{(2)\dagger} + c_J^{(3)\dagger} c_{J'}^{(4)\dagger} c_{K'}^{(1)\dagger} c_K^{(2)\dagger}\big) + \overline{\mathcal{O}}_{J,J',K,K'}$$

$$= \mathcal{R}_1\mathcal{R}_2\mathcal{T}_1\mathcal{T}_2\big(c_K^{(1)\dagger} c_{K'}^{(2)\dagger} c_{J'}^{(3)\dagger} c_J^{(4)\dagger} + c_{K'}^{(1)\dagger} c_K^{(2)\dagger} c_{J'}^{(3)\dagger} c_J^{(4)\dagger} + c_K^{(1)\dagger} c_{K'}^{(2)\dagger} c_J^{(3)\dagger} c_{J'}^{(4)\dagger} + c_{K'}^{(1)\dagger} c_K^{(2)\dagger} c_J^{(3)\dagger} c_{J'}^{(4)\dagger}\big) + \overline{\mathcal{O}}_{J,J',K,K'}, \tag{A18}$$

where we have grouped the terms that cannot result in a fourfold coincidence in the term $\overline{\mathcal{O}}_{J,J',K,K'}$. Note that if $J = J'$ and $K = K'$, we have

$$\mathcal{O}_{J,J,K,K} = 4\mathcal{R}_1\mathcal{R}_2\mathcal{T}_1\mathcal{T}_2\big(c_K^{(1)\dagger} c_K^{(2)\dagger} c_J^{(3)\dagger} c_J^{(4)\dagger}\big) + \overline{\mathcal{O}}_{J,J,K,K}. \tag{A19}$$

Our notation for the states generated by these operators will be the following:

$$c_K^{(1)\dagger} c_{K'}^{(2)\dagger} c_J^{(3)\dagger} c_{J'}^{(4)\dagger}|\text{vac}\rangle = |K, K', J, J'\rangle. \tag{A20}$$

We can then see that

$$\mathcal{O}_{J,J',K,K'}|\text{vac}\rangle = \mathcal{R}_1\mathcal{R}_2\mathcal{T}_1\mathcal{T}_2\big(|K, K', J', J\rangle + |K', K, J', J\rangle + |K, K', J, J'\rangle + |K', K, J, J'\rangle\big) + \overline{\mathcal{O}}_{J,J',K,K'}|\text{vac}\rangle, \tag{A21}$$

where the latter term will be excluded by postselecting on fourfold coincidences.

b. Output state and filtering

Recall Eq. (A11), which is the four-photon state generated by the source. After propagating through the beam splitters, the part of the state with a photon in each of the four outputs can be written as

$$|IV\rangle = \mathcal{N}\big(\beta_1^2 \mathcal{O}_{S0,S0,I1,I1} + \beta_2^2 \mathcal{O}_{S1,S1,I0,I0} + 2\beta_1\beta_2 \mathcal{O}_{S0,S1,I0,I1}\big)|\text{vac}\rangle, \tag{A22}$$

with $\mathcal{N}$ defined in (A12). Using (A21) we have

$$|IV\rangle = \mathcal{N}\big(\mathcal{R}_1\mathcal{R}_2\mathcal{T}_1\mathcal{T}_2\big[4\beta_1^2 |I1, I1, S0, S0\rangle + 4\beta_2^2 |I0, I0, S1, S1\rangle + 2\beta_1\beta_2\big(|I0, I1, S1, S0\rangle + |I1, I0, S1, S0\rangle \\ + |I0, I1, S0, S1\rangle + |I1, I0, S0, S1\rangle\big)\big] + \big[\beta_1^2 \mathcal{O}_{S0,S0,I1,I1} + \beta_2^2 \mathcal{O}_{S1,S1,I0,I0} + 2\beta_1\beta_2 \mathcal{O}_{S0,S1,I0,I1}\big]|\text{vac}\rangle\big) \tag{A23}$$

and we define

$$|IV'\rangle = \mathcal{N}'\big[4\beta_1^2 |I1, I1, S0, S0\rangle + 4\beta_2^2 |I0, I0, S1, S1\rangle \\ + 2\beta_1\beta_2\big(|I0, I1, S1, S0\rangle + |I1, I0, S1, S0\rangle + |I0, I1, S0, S1\rangle + |I1, I0, S0, S1\rangle\big)\big], \tag{A24}$$

where $|IV'\rangle$ is the state describing fourfold coincidence events only. We separate the signal or idler and frequency bin (0/1) degrees of freedom by writing, e.g., $|S0\rangle$, explicitly as a composite system with two degrees of freedom $|S\rangle|0\rangle$. In this notation

we have

$$|IV'\rangle = \mathcal{N}'\left[4\beta_1^2\,|1,1,0,0\rangle + 4\beta_2^2\,|0,0,1,1\rangle + 2\beta_1\beta_2(|0,1,1,0\rangle + |1,0,1,0\rangle + |0,1,0,1\rangle + |1,0,0,1\rangle)\right]|I,I,S,S\rangle \quad \text{(A25)}$$

and clearly, if we trace over S and I, we have a pure state in the frequency bin degree of freedom. Finally, we also postselect on frequency bin 1 in the herald detector, which we take to be detector 4. Doing this we are left with

$$|IV'\rangle = \mathcal{N}''\left[4\beta_2^2\,|0,0,1\rangle_{123} + 2\beta_1\beta_2(|0,1,0\rangle_{123} + |1,0,0\rangle_{123})\right]|1\rangle_4, \quad \text{(A26)}$$

$$\mathcal{N}'' = \frac{1}{\sqrt{16|\beta_2|^4 + 8|\beta_1|^2|\beta_2|^2}}. \quad \text{(A27)}$$

Now if we set the pump powers such that $\beta_1\beta_2 = 2\beta_1^2$, we have

$$|IV'\rangle = \frac{1}{\sqrt{3}}(|0,0,1\rangle + |0,1,0\rangle + |1,0,0\rangle)_{123}\,|1\rangle_4, \quad \text{(A28)}$$

which is a W state in ports 1,2,3. Notice one could also use the pump phases to add a relative phase to one of the three terms, but not arbitrary relative phases between the three terms; in principle it seems this could be done by adding a frequency-dependent phase shift to one of the paths. Of course, the relative amplitudes between the terms can be modified; although the state is not completely general, the tunability in (A26) is sufficient to construct a W state that is suitable for superdense coding and perfect teleportation [29].

c. W rate

Many of the photon-pair pairs generated by the microring source do not result in fourfold coincidences. We can find the fraction of photons that remain by computing the overlap between $|IV'\rangle$ in (A26), which is the postselected state, and $|IV\rangle$ in (A23), which is the full four-photon state. We find

$$|\langle IV|IV'\rangle|^2 = |\mathcal{N}|^2|\mathcal{N}''|^2|\mathcal{R}_1\mathcal{R}_2\mathcal{T}_1\mathcal{T}_2|^2$$
$$\times \left(16|\beta_2|^4 + 8|\beta_1|^2|\beta_2|^2\right)^2 \quad \text{(A29)}$$
$$= \left(\frac{1}{4|\beta_1|^4 + 4|\beta_2|^4 + 4|\beta_1|^2|\beta_2|^2}\right)$$
$$\times \left(\frac{1}{16|\beta_2|^4 + 8|\beta_1|^2|\beta_2|^2}\right)|\mathcal{R}_1\mathcal{R}_2\mathcal{T}_1\mathcal{T}_2|^2$$
$$\times \left(16|\beta_2|^4 + 8|\beta_1|^2|\beta_2|^2\right)^2. \quad \text{(A30)}$$

Putting $\mathcal{R}_1 = \mathcal{R}_2 = \mathcal{T}_1 = \mathcal{T}_2 = \frac{1}{\sqrt{2}}$, which optimizes rate of W states, we have

$$|\langle IV|IV'\rangle|^2 = \left(\frac{16|\beta_2|^4 + 8|\beta_1|^2|\beta_2|^2}{4|\beta_1|^4 + 4|\beta_2|^4 + 4|\beta_1|^2|\beta_2|^2}\right)\frac{1}{16} \quad \text{(A31)}$$
$$= \left(\frac{2|\beta_2|^4 + |\beta_1|^2|\beta_2|^2}{|\beta_1|^4 + |\beta_2|^4 + |\beta_1|^2|\beta_2|^2}\right)\frac{1}{8}. \quad \text{(A32)}$$

If we put $2\beta_2 = \beta_1$, which gives the W state of Eq. (A28), we have

$$|\langle IV|IV'\rangle|^2 = \left(\frac{6}{21}\right)\frac{1}{8} = \frac{1}{28}. \quad \text{(A33)}$$

That is, of the pairs of pairs generated in the source, $\frac{1}{28}$ lead to fourfold coincidences; we expect

$$\mathcal{R}_W = \mathcal{R}_{IV}/28, \quad \text{(A34)}$$

where $\mathcal{R}_W$ is the rate of W states and $\mathcal{R}_{IV}$ is the rate of photon-pair pairs from the source.

2. Four-photon GHZ state

a. Sources

Here we take two SFWM sources in the pair generation regime, with the resonances configured as shown in Fig. 1. The nonlinear Hamiltonian describing each source can be taken to be

$$H_{\text{NL}}(t) = \hbar\Gamma\alpha(t)a_{S0}^\dagger a_{I0}^\dagger + \hbar\Gamma'\alpha'(t)a_{S1}^\dagger a_{I1}^\dagger + \text{H.c.} \quad \text{(A35)}$$

Neglecting time-ordering corrections, the state generated by this Hamiltonian is

$$|\psi\rangle = e^{-\frac{i}{\hbar}\int_{t_0}^t dt' H_{\text{NL}}(t')}|\text{vac}\rangle \quad \text{(A36)}$$
$$= e^{-i\int_{t_0}^t dt'[\Gamma\alpha(t')a_{S0}^\dagger a_{I0}^\dagger + \Gamma'\alpha'(t')a_{S1}^\dagger a_{I1}^\dagger + \text{H.c.}]}|\text{vac}\rangle \quad \text{(A37)}$$
$$= e^{\left\{-i\Gamma\left(\int_{t_0}^t dt'\alpha(t')\right)a_{S0}^\dagger a_{I0}^\dagger - i\Gamma\left(\int_{t_0}^t dt'\alpha'(t')\right)a_{S1}^\dagger a_{I1}^\dagger\right\}-\text{H.c.}}|\text{vac}\rangle \quad \text{(A38)}$$
$$\equiv e^{\beta C_{II}^\dagger - \text{H.c.}}|\text{vac}\rangle, \quad \text{(A39)}$$

where now

$$C_{II}^\dagger = \frac{1}{\beta}\left\{-i\Gamma\left(\int_{t_0}^t dt'\alpha(t')\right)a_{S0}^\dagger a_{I0}^\dagger\right.$$
$$\left.-i\Gamma\left(\int_{t_0}^t dt'\alpha'(t')\right)a_{S1}^\dagger a_{I1}^\dagger\right\} \quad \text{(A40)}$$
$$\equiv \frac{1}{\beta}\{\beta_1 a_{S0}^\dagger a_{I0}^\dagger + \beta_2 a_{S1}^\dagger a_{I1}^\dagger\}. \quad \text{(A41)}$$

Here $|\beta|^2 = |\beta_1|^2 + |\beta_2|^2$ is the probability of generating a pair per pump pulse and $C_{II}^\dagger|\text{vac}\rangle$ is a normalized two-photon state. If we set $\beta_2 = \beta_1 e^{i\phi}$, then the two-photon state corresponds to a frequency-bin-encoded Bell state of the form

$$|\Phi\rangle = \frac{1}{\sqrt{2}}(a_{S0}^\dagger a_{I0}^\dagger + e^{i\phi}a_{S1}^\dagger a_{I1}^\dagger)|\text{vac}\rangle \quad \text{(A42)}$$
$$= \frac{1}{\sqrt{2}}(|00\rangle + e^{i\phi}|11\rangle), \quad \text{(A43)}$$

where the two qubits are the signal and idler photons and their logical states are encoded in the frequency bins in which they are generated.

Returning to the more general case, we consider the low pair generation probability regime, such that the state generated by each source is approximately

$$|\psi\rangle = |vac\rangle + \beta C_{II}^{\dagger} |vac\rangle \tag{A44}$$

$$= |vac\rangle + (\beta_1 a_{S0}^{\dagger} a_{I0}^{\dagger} + \beta_2 a_{S1}^{\dagger} a_{I1}^{\dagger}) |vac\rangle . \tag{A45}$$

We neglect the four-photon term in Eq. (A45) because such terms will not result in fourfold coincidences.

b. Manipulation

We now discuss the manipulation of the photons in the GHZ device (see Fig. 3). We begin with two-photon pair sources configured as described above [see Eq. (A45)]. We label the two spatial modes associated with the sources path 1 and 4. The state generated by the two rings is approximately

$$|\psi\rangle = \left[|vac\rangle + \left(\beta_1 a_{S0}^{\dagger(1)} a_{I0}^{\dagger(1)} + \beta_2 a_{S1}^{\dagger(1)} a_{I1}^{\dagger(1)} \right) |vac\rangle \right]$$
$$\otimes \left[|vac\rangle + \left(\beta_3 a_{S0}^{\dagger(4)} a_{I0}^{\dagger(4)} + \beta_4 a_{S1}^{\dagger(4)} a_{I1}^{\dagger(4)} \right) |vac\rangle \right] \tag{A46}$$

$$= |\psi_{0,2}\rangle + \left(\beta_1 a_{S0}^{\dagger(1)} a_{I0}^{\dagger(1)} + \beta_2 a_{S1}^{\dagger(1)} a_{I1}^{\dagger(1)} \right) |vac\rangle$$
$$\otimes \left(\beta_3 a_{S0}^{\dagger(4)} a_{I0}^{\dagger(4)} + \beta_4 a_{S1}^{\dagger(4)} a_{I1}^{\dagger(4)} \right) |vac\rangle , \tag{A47}$$

where in (A47) we have grouped the terms that result in the generation of no photons or photon pairs in $|\psi_{0,2}\rangle$. After each source, the signal and idler photons are separated using an add-drop filter; the path taken by signal photons remains unchanged, while idler photons are routed into a new path. The state is then

$$|\psi\rangle = |\psi_{0,2}\rangle + \left(\beta_1 a_{S0}^{\dagger(1)} a_{I0}^{\dagger(2)} + \beta_2 a_{S1}^{\dagger(1)} a_{I1}^{\dagger(2)} \right) |vac\rangle$$
$$\otimes \left(\beta_3 a_{S0}^{\dagger(4)} a_{I0}^{\dagger(3)} + \beta_4 a_{S1}^{\dagger(4)} a_{I1}^{\dagger(3)} \right) |vac\rangle . \tag{A48}$$

Next, paths 2 and 3 are mixed at an add-drop filter. The ring is resonant with the frequency bin $I1$, so photons in bin $I0$

remain in the same path, while photons in $I1$ are swapped. That is, the add-drop effects the transformation

$$a_{I0}^{\dagger(2)} \to a_{I0}^{\dagger(2)}, \tag{A49}$$

$$a_{I0}^{\dagger(3)} \to a_{I0}^{\dagger(3)}, \tag{A50}$$

$$a_{I1}^{\dagger(2)} \to a_{I1}^{\dagger(3)}, \tag{A51}$$

$$a_{I1}^{\dagger(3)} \to a_{I1}^{\dagger(2)}, \tag{A52}$$

so the state becomes

$$|\psi\rangle = |\psi_{0,2}\rangle + \left(\beta_1 a_{S0}^{\dagger(1)} a_{I0}^{\dagger(2)} + \beta_2 a_{S1}^{\dagger(1)} a_{I1}^{\dagger(3)} \right) |vac\rangle$$
$$\otimes \left(\beta_3 a_{S0}^{\dagger(4)} a_{I0}^{\dagger(3)} + \beta_4 a_{S1}^{\dagger(4)} a_{I1}^{\dagger(2)} \right) |vac\rangle . \tag{A53}$$

Expanding the tensor product we have

$$|\psi\rangle = |\psi_{0,2}\rangle + \left(\beta_1 \beta_4 a_{S0}^{\dagger(1)} a_{I0}^{\dagger(2)} a_{S1}^{\dagger(4)} a_{I1}^{\dagger(2)} \right.$$
$$+ \beta_2 \beta_3 a_{S1}^{\dagger(1)} a_{I1}^{\dagger(3)} a_{S0}^{\dagger(4)} a_{I0}^{\dagger(3)} \right) |vac\rangle$$
$$+ \left(\beta_1 \beta_3 a_{S0}^{\dagger(1)} a_{I0}^{\dagger(2)} a_{S0}^{\dagger(4)} a_{I0}^{\dagger(3)} \right.$$
$$+ \beta_2 \beta_4 a_{S1}^{\dagger(1)} a_{I1}^{\dagger(3)} a_{S1}^{\dagger(4)} a_{I1}^{\dagger(2)} \right) |vac\rangle . \tag{A54}$$

Only the third term can lead to fourfold coincidences, while the first two cannot. We focus on the last term

$$|GHZ\rangle = \mathcal{N} \left(\beta_1 \beta_3 a_{S0}^{\dagger(1)} a_{I0}^{\dagger(2)} a_{I0}^{\dagger(3)} a_{S0}^{\dagger(4)} \right.$$
$$+ \beta_2 \beta_4 a_{S1}^{\dagger(1)} a_{I1}^{\dagger(2)} a_{I1}^{\dagger(3)} a_{S1}^{\dagger(4)} \right) |vac\rangle \tag{A55}$$

$$= \mathcal{N} \left(\beta_1 \beta_3 |0000\rangle |SIIS\rangle + \beta_2 \beta_4 |1111\rangle |SIIS\rangle \right) \tag{A56}$$

$$= \mathcal{N} \left(\beta_1 \beta_3 |0000\rangle + \beta_2 \beta_4 |1111\rangle \right) , \tag{A57}$$

where we have introduced the same notation used above to distinguish the frequency bin and signal or idler degrees of freedom and traced over the latter. We have a four-photon GHZ state with arbitrary relative amplitude and phase between the two terms.

---

[1] M. Pont, G. Corrielli, A. Fyrillas, I. Agresti, G. Carvacho, N. Maring, P.-E. Emeriau, F. Ceccarelli, R. Albiero, P. H. D. Ferreira, N. Somaschi, J. Senellart, I. Sagnes, M. Morassi, A. Lemaitre, P. Senellart, F. Sciarrino, M. Liscidini, N. Belabas, and R. Osellame, High-fidelity generation of four-photon GHZ states on-chip, arXiv:2211.15626.

[2] P. Imany, J. A. Jaramillo-Villegas, M. S. Alshaykh, J. M. Lukens, O. D. Odele, A. J. Moore, D. E. Leaird, M. Qi, and A. M. Weiner, High-dimensional optical quantum logic in large operational spaces, npj Quantum Inf. **5**, 59 (2019).

[3] M. Hillery, V. Bužek, and A. Berthiaume, Quantum secret sharing, Phys. Rev. A **59**, 1829 (1999).

[4] K. Azuma, K. Tamaki, and H.-K. Lo, All-photonic quantum repeaters, Nat. Commun. **6**, 6787 (2015).

[5] J.-W. Pan, M. Daniell, S. Gasparoni, G. Weihs, and A. Zeilinger, Experimental demonstration of four-photon entanglement and high-fidelity teleportation, Phys. Rev. Lett. **86**, 4435 (2001).

[6] E. Meyer-Scott, N. Prasannan, I. Dhand, C. Eigner, V. Quiring, S. Barkhofen, B. Brecht, M. B. Plenio, and C. Silberhorn, Scalable generation of multiphoton entangled states by active feed-forward and multiplexing, Phys. Rev. Lett. **129**, 150501 (2022).

[7] N. Bergamasco, M. Menotti, J. E. Sipe, and M. Liscidini, Generation of path-encoded Greenberger-Horne-Zeilinger states, Phys. Rev. Appl. **8**, 054014 (2017).

[8] M. Li, C. Li, Y. Chen, L.-T. Feng, L. Yan, Q. Zhang, J. Bao, B.-H. Liu, X.-F. Ren, J. Wang, S. Wang, Y. Gao, X. Hu, Q. Gong, and Y. Li, On-chip path encoded photonic quantum toffoli gate, Photon. Res. **10**, 1533 (2022).

[9] J. Bao, Z. Fu, T. Pramanik, J. Mao, Y. Chi, Y. Cao, C. Zhai, Y. Mao, T. Dai, X. Chen, X. Jia, L. Zhao, Y. Zheng, B. Tang, Z. Li, J. Luo, W. Wang, Y. Yang, Y. Peng, D. Liu *et al.*, Very-large-scale integrated quantum graph photonics, Nat. Photon. **17**, 573 (2023).

[10] B. Fang, M. Menotti, M. Liscidini, J. E. Sipe, and V. O. Lorenz, Three-photon discrete-energy-entangled *w* state in an optical fiber, Phys. Rev. Lett. **123**, 070508 (2019).

[11] M. Menotti, L. Maccone, J. E. Sipe, and M. Liscidini, Generation of energy-entangled w states via parametric fluorescence in integrated devices, Phys. Rev. A **94**, 013845 (2016).

[12] P. Imany, J. A. Jaramillo-Villegas, O. D. Odele, K. Han, D. E. Leaird, J. M. Lukens, P. Lougovski, M. Qi, and A. M. Weiner, 50-GHz-spaced comb of high-dimensional frequency-bin entangled photons from an on-chip silicon nitride microresonator, Opt. Express **26**, 1825 (2018).

[13] C. Reimer, M. Kues, P. Roztocki, B. Wetzel, F. Grazioso, B. E. Little, S. T. Chu, T. Johnston, Y. Bromberg, L. Caspani, D. J. Moss, and R. Morandotti, Generation of multiphoton entangled quantum states by means of integrated frequency combs, Science **351**, 1176 (2016).

[14] M. Kues, C. Reimer, P. Roztocki, L. R. Cortés, S. Sciara, B. Wetzel, Y. Zhang, A. Cino, S. T. Chu, B. E. Little, D. J. Moss, L. Caspani, J. Azaña, and R. Morandotti, On-chip generation of high-dimensional entangled quantum states and their coherent control, Nature (London) **546**, 622 (2017).

[15] M. Liscidini and J. E. Sipe, Scalable and efficient source of entangled frequency bins, Opt. Lett. **44**, 2625 (2019).

[16] M. Clementi, F. A. Sabattoli, M. Borghi, L. Gianini, N. Tagliavacche, H. E. Dirani, L. Youssef, N. Bergamasco, C. Petit-Etienne, E. Pargon, J. E. Sipe, M. Liscidini, C. Sciancalepore, M. Galli, and D. Bajoni, Programmable frequency-bin quantum states in a nano-engineered silicon device, Nat. Commun. **14**, 176 (2023).

[17] S. Seshadri, H.-H. Lu, D. E. Leaird, A. M. Weiner, and J. M. Lukens, Complete frequency-bin bell basis synthesizer, Phys. Rev. Lett. **129**, 230505 (2022).

[18] J. B. Christensen, J. G. Koefoed, K. Rottwitt, and C. J. McKinstrie, Engineering spectrally unentangled photon pairs from nonlinear microring resonators by pump manipulation, Opt. Lett. **43**, 859 (2018).

[19] Z. Vernon, M. Menotti, C. C. Tison, J. A. Steidle, M. L. Fanto, P. M. Thomas, S. F. Preble, A. M. Smith, P. M. Alsing, M. Liscidini, and J. E. Sipe, Truly unentangled photon pairs without spectral filtering, Opt. Lett. **42**, 3638 (2017).

[20] D. Grassani, A. Simbula, S. Pirotta, M. Galli, M. Menotti, N. C. Harris, T. Baehr-Jones, M. Hochberg, C. Galland, M. Liscidini, and D. Bajoni, Energy correlations of photon pairs generated by

a silicon microring resonator probed by stimulated four wave mixing, Sci. Rep. **6**, 23564 (2016).

[21] L. G. Helt, Z. Yang, M. Liscidini, and J. E. Sipe, Spontaneous four-wave mixing in microring resonators, Opt. Lett. **35**, 3006 (2010).

[22] L. G. Helt, M. Liscidini, and J. E. Sipe, How does it scale? Comparing quantum and classical nonlinear optical processes in integrated devices, J. Opt. Soc. Am. B **29**, 2199 (2012).

[23] T. Onodera, M. Liscidini, J. E. Sipe, and L. G. Helt, Parametric fluorescence in a sequence of resonators: An analogy with dicke superradiance, Phys. Rev. A **93**, 043837 (2016).

[24] J.-W. Pan, D. Bouwmeester, M. Daniell, H. Weinfurter, and A. Zeilinger, Experimental test of quantum nonlocality in three-photon Greenberger–Horne–Zeilinger entanglement, Nature (London) **403**, 515 (2000).

[25] J.-C. Hao, C.-F. Li, and G.-C. Guo, Controlled dense coding using the Greenberger-Horne-Zeilinger state, Phys. Rev. A **63**, 054301 (2001).

[26] F. Hahn, J. de Jong, and A. Pappa, Anonymous quantum conference key agreement, PRX Quantum **1**, 020325 (2020).

[27] W. Dür, G. Vidal, and J. I. Cirac, Three qubits can be entangled in two inequivalent ways, Phys. Rev. A **62**, 062314 (2000).

[28] C. Zhu, F. Xu, and C. Pei, W-state analyzer and multi-party measurement-device-independent quantum key distribution, Sci. Rep. **5**, 17449 (2015).

[29] P. Agrawal and A. Pati, Perfect teleportation and superdense coding with *w* states, Phys. Rev. A **74**, 062320 (2006).

[30] X. Yang, M. qiang Bai, and Z. wen Mo, Controlled dense coding with the w state, Int. J. Theor. Phys. **56**, 3525 (2017).

[31] S.-B. Zheng, Splitting quantum information via W states, Phys. Rev. A **74**, 054303 (2006).

[32] V. Lipinska, G. Murta, and S. Wehner, Anonymous transmission in a noisy quantum network using the *W* state, Phys. Rev. A **98**, 052320 (2018).

[33] P. Faist, S. Nezami, V. V. Albert, G. Salton, F. Pastawski, P. Hayden, and J. Preskill, Continuous symmetries and approximate quantum error correction, Phys. Rev. X **10**, 041018 (2020).

[34] M. Erhard, M. Malik, M. Krenn, and A. Zeilinger, Experimental Greenberger–Horne–Zeilinger entanglement beyond qubits, Nat. Photon. **12**, 759 (2018).

[35] M. Krenn, X. Gu, and A. Zeilinger, Quantum experiments and graphs: Multiparty states as coherent superpositions of perfect matchings, Phys. Rev. Lett. **119**, 240403 (2017).